

CHAPTER ONE HUNDRED THIRTY

ON PREDICTING INFRAGRAVITY ENERGY IN THE SURF ZONE

Asbury H. Sallenger, Jr.* and Robert A. Holman**

Abstract

Flow data were obtained in the surf zone across a barred profile during a storm. RMS cross-shore velocities due to waves in the infragravity band (wave periods greater than 20 s) had maxima in excess of 0.5 m/s over the bar crest. For comparison to measured spectra, synthetic spectra of cross-shore flow were computed using measured nearshore profiles. The synthetic spectra were calculated assuming a white runup spectrum of mode-4 edge waves of unit amplitude, although the results would be essentially the same for standing waves or any edge-wave mode above 2. The structure, in the infragravity band, of these synthetic spectra corresponded reasonably well with the structure of the measured spectra. Total variances of measured cross-shore flow within the infragravity band were nondimensionalized by dividing by total infragravity variances of synthetic spectra. These nondimensional variances were independent of distance offshore and increased with the square of the breaker height. Thus, cross-shore flow due to infragravity waves can be estimated with knowledge of the nearshore profile and incident wave conditions.

Introduction

Waves in the infragravity band, usually defined as wave periods greater than 20 s, can be energetic in the surf zone when offshore waves are large (for example, Holman et al., 1978; Wright et al., 1979; Guza and Thornton, 1981; Holman, 1981; Holman and Sallenger, in press). In fact, within the swash and inner surf zones, energy in the infragravity band has been observed to exceed, sometimes greatly, the energy of waves in the incident band, wave periods less than 20 s. In view of the significance of energy in the infragravity band, flows caused by infragravity waves are likely important to sediment transport in the surf zone (Bowen and Inman, 1971; Short, 1975; Wright et al., 1979; Wright et al., 1982; Sallenger et al., in press). In this paper, we focus on the prediction of the magnitude of cross-shore flows due to infragravity waves.

* U.S. Geological Survey, Menlo Park, CA 94025

**Oregon State University, Corvallis, OR 97331

Several studies have tried to quantify the relationship between the magnitude of waves in the infragravity band and parameters characterizing offshore wave conditions. Guza and Thornton (1981) found that significant swash oscillations due to infragravity waves increased with increasing offshore wave height. Using a much larger data set, Holman and Sallenger (in press) showed that infragravity swash oscillations could be predicted better by the Iribarren Number

$$\xi_o = \tan\beta (H_o/L_o)^{-0.5} \quad (1)$$

where β is foreshore slope and H_o/L_o is deep-water wave steepness.

Runup data, such as used by the two studies discussed above, are particularly useful in determining the relationship between the magnitude of infragravity waves at the shoreline and offshore wave characteristics. This is because infragravity waves in the surf zone have the cross-shore structure of standing waves or high-mode edge waves (Suhayda, 1974; Holman, 1981). Measurements at the shoreline, such as runup, are not affected by offshore decay of energy or by offshore nodal positions which vary with frequency. To use offshore measurements, such as measurements of flow, we must account for the effects of the standing wave structure.

In the present study, cross-shore flow data were obtained across the surf zone during a storm. To account for offshore position of the flow measurements, we nondimensionalized measured variances of cross-shore flow in the infragravity band by computed variances based on a white runup spectrum of edge waves (or standing waves) of unit amplitude. We will show that the nondimensional variances are predictable by incident wave characteristics.

In the following section, we discuss the significance of nondimensional flow variances and how the variances were calculated. After presenting the experimental methods and setting, we discuss measured cross-shore flow data and how flow varied over the barred profile during the storm. Next, we show how well synthetic infragravity spectra, based on the white runup spectrum, matched the measured spectra, and, similarly, how well total variances in the infragravity band of the synthetic spectra matched that of the measured spectra. Finally, we show how nondimensional variances varied with incident wave conditions.

Theory

As discussed above, a difficulty of interpreting data from fixed locations in the surf zone is that the waves in the infragravity band appear to be standing. The shape of the infragravity part of the spectrum is strongly dependent upon the cross-shore position at which the record was obtained. In order to interpret the offshore flow data, we have calculated synthetic spectra based on a white runup spectrum of mode-4 edge waves with unit shoreline amplitude. The results would be essentially the same for standing waves or edge

waves of any mode above 2. The calculations were performed as described in Holman (1981). Cross-shore flow variances were found numerically for different distances offshore and for different frequencies within the infragravity band. Using these calculated variances, synthetic spectra were computed for distances offshore corresponding to measured spectra. These synthetic spectra offer a means to interpret the measured infragravity spectra in that valleys and peaks associated with standing wave motions can be directly compared to measured spectra.

For a particular distance offshore, we can also compare total variances in the infragravity band of measured and synthetic spectra. A nondimensionalized infragravity variance is given by

$$\lambda^2 = \frac{\int_0^{\zeta} U_{vr}^m(f) df}{\int_0^{\zeta} U_{vr}^c(f) df} \quad (2)$$

where $U_{vr}^m(f)$ and $U_{vr}^c(f)$ are measured and computed cross-shore velocity spectra respectively, and ζ is the frequency separating incident and infragravity bands. As mentioned above, ζ is usually taken rather arbitrarily as 0.05 Hz. Here, we have defined ζ for each incident wave condition by determining, visually, the low frequency side of the dominant incident wave peak. Periods of incident wave peaks varied from 10 to 18 s. Using a 20 s (0.05 Hz) cutoff for the spectrum with the 10 s dominant incident wave may underestimate the amount of energy in the infragravity band.

λ^2 is a measure of the level of energy in the infragravity band, and is independent of position offshore and profile configuration. Thus, λ^2 can be directly compared to offshore wave parameters. However, λ^2 assumes a white runup spectrum and would not be a useful quantity if the runup spectrum had only one, or a few, energetic frequencies in the infragravity band. It is possible that if a broad band of infragravity energy is forced when offshore waves become large, λ^2 may be a useful quantity even if the runup spectrum is not uniformly white. Below we find reasonable correspondence, for data obtained during a storm, between λ^2 and a parameter characterizing incident wave conditions.

Experiment Setting and Methods

The experiment, known as DUCK82, was conducted during October 1982 at the Field Research Facility (FRF) of the US Army Corps of Engineers in Duck, North Carolina. The FRF is located on a long straight beach of a barrier island. Mason et al. (this volume) present details of the experiment setting, and introduce papers on other investigations conducted during the DUCK82 experiment.

Flow data were obtained using the USGS sled system (described in detail in Sallenger et al., 1983). The system consists of an instrumented sled that was towed along the bottom, both offshore and onshore, with a double-drum winch and triangular-line arrangement. Three electromagnetic current meters (Marsh-McBirney model 512) in a

vertical array and a pressure sensor were mounted onto the frame of the sled and the data were telemetered to a shore receiving station. The nearshore profile was measured using an infrared rangefinder on the beach and optical prisms mounted on top of the sled's mast. The sled system was set up 500 m north of the FRF pier, presumably outside the influence of the pier (Mason et al., this volume).

The flow data discussed here were obtained with a current meter mounted on the sled 1 m above the bottom. For a given day, records were obtained at five to eight locations across the surf zone. Each record was 34.1 minutes long. A set of records was obtained around high tide to minimize depth variations during the runs.

Results

Much of the cross-shore flow data discussed here were taken during a storm, October 10-12, 1982. The remainder of the data were taken immediately following the peak of the storm, Oct. 13, and on a relatively calm day when nearshore morphology was not highly three-dimensional, Oct. 20. Details of the meteorological and wave characteristics of the storm and post-storm period are given in Mason et al. (this volume). An example of the bar response during the storm is shown in Fig. 1A. The bar migrated offshore at rates up to 2.2 m/hr. Following the storm, the bar morphology developed into a classic example of a crescentic bar. Mason et al. (this volume) and Sallenger et al. (in press) discuss the storm-induced response of the nearshore morphology.

RMS cross-shore flows due to waves in the infragravity band exceeded 0.5 m/s (Fig. 1B). We defined infragravity RMS cross-shore flow as

$$U_{rms_ig} = \left(\int_0^{\zeta} U_{vr}^m(f) df \right)^{0.5} \quad (3)$$

Note that maxima in cross-shore flow occurred at the crest of the bar. These flow maxima are evidently the result of mass transport over the shallow water of the bar crest.

Relative magnitudes of cross-shore flows due to infragravity waves and incident waves are shown in Figure 1C. At places within the inner surf zone, cross-shore flow variances in the infragravity band approached or exceeded variances in the incident band. Note that for everywhere on the profile, ratios of variances in the infragravity band to those in the incident band for October 12 are greater than ratios for October 10. Since variances in the incident band are limited by wave breaking (the breaker zone occurring several hundred meters farther offshore than our seawardmost measurement location), Figure 1C indicates that infragravity energy became increasingly important during the two days. Below, we will try to quantify a relationship between infragravity energy and characteristics of offshore waves.

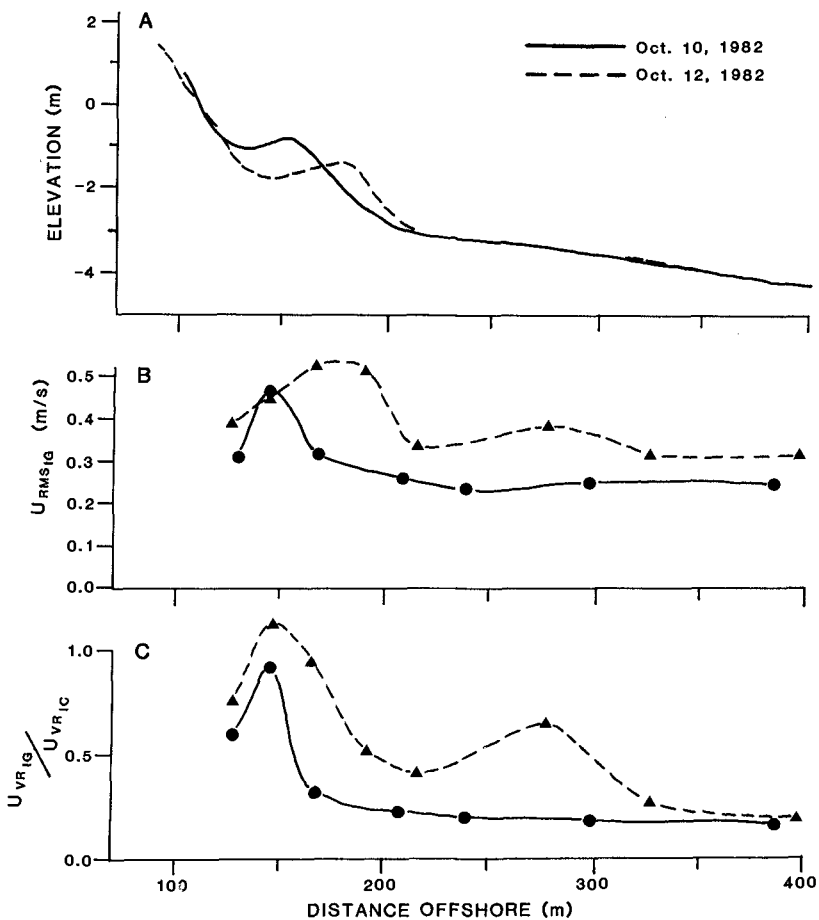


Figure 1. A. Nearshore profiles measured with the USGS sled system for two of the storm days. B. Measured RMS cross-shore flows of the infragravity band. C. Ratios of variances of the infragravity band to variances of the incident band.

We present four spectra from a single day (Figs. 2 and 3) to illustrate the correspondence between measured and synthetic spectra. The locations of each measurement station on the nearshore profile are shown in Figure 4. As discussed above, the synthetic spectra are based on a white runup spectrum of unit amplitude. The measured spectral structures agree reasonably well with the synthetic structures. For example, spectral valleys, which indicate positions of zero crossings (nodes), of the measured spectra coincide closely with valleys of synthetic spectra. Energy levels of synthetic spectra were adjusted by moving the spectra vertically in order to fit the lower energy peaks of the measured spectrum. For a given set of records, all obtained on the same day under basically the same incident wave conditions, the calculated spectra are moved vertically the same amount. Any dominant peaks in the measured spectra would rise above the synthetic spectra. (Alternatively, the energy levels of synthetic spectra could have been adjusted by multiplying by the mean of λ^2 for a given day which would yield a best fit between the measured and synthetic spectra). Much of the infragravity energy in the measured spectra fits the synthetic spectra; however, at some frequencies energy in the measured spectra exceeds the energy in the synthetic spectra. At these frequencies, there should be peaks in the runup spectrum, that is, the runup spectrum was not white. These dominant peaks appear to have been induced by the bar offshore; their significance will be discussed elsewhere.

For a particular distance offshore, we define a synthetic infragravity variance as

$$U_{vr,ig}^c = \overline{\lambda^2} \int_0^{\zeta} U_{vr}^c(f) df \tag{4}$$

where the overbar indicates that λ^2 is averaged for all offshore positions for a given day. A measured infragravity variance is given by the numerator of equation 2. In Figure 5, we compare measured and synthetic infragravity variances for different distances offshore. Only two days are shown, but the correspondence is similar for all days. Since the shapes of the curves for each day are nearly the same, λ^2 (equation 2) is roughly constant for a given day and independent of distance offshore.

For five different days with greatly varying incident wave conditions, values of λ^2 were calculated. In Figure 6 we show how mean λ^2 for a given day varied with the square of the offshore significant breaker height, H_b . H_b was calculated from offshore wave characteristics using Komar and Gaughan (1973). There is good correspondence between H_b^2 and λ^2 . Linear regression gives

$$\overline{\lambda^2} = 0.45 H_b^2 - 0.60 \tag{5}$$

with $r = 0.99$. For equation 4 to be dimensionally correct, a factor of unity with dimensions of m^{-2} is multiplied times the slope.

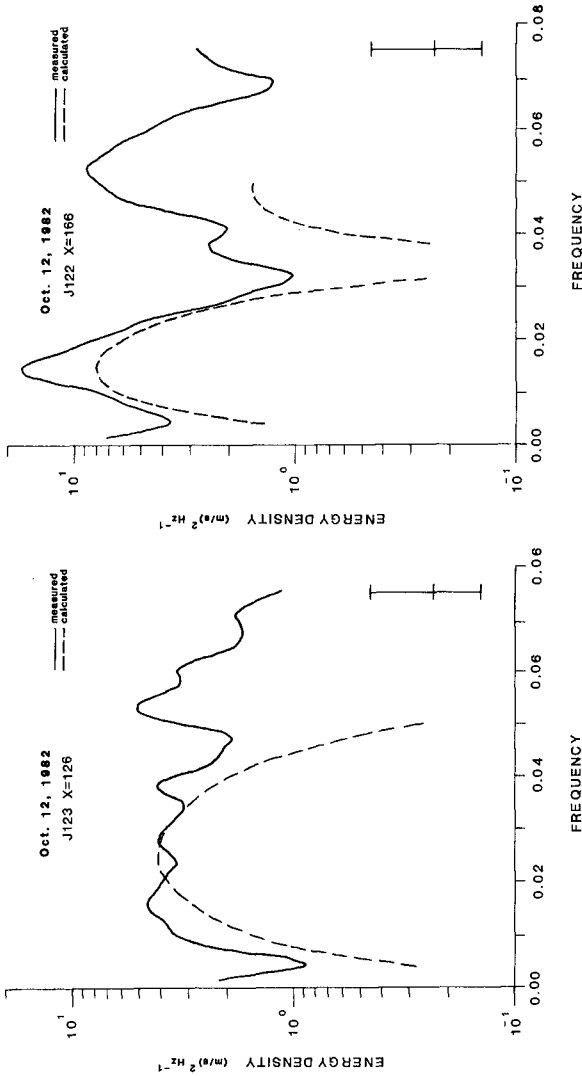


Figure 2. Surf-zone spectra from October 12, 1982. X indicates distance offshore in meters from a baseline; the shoreline relative to this baseline is about 110 m. The number preceded by the J is the run number. 95% confidence limits are shown. The location of each measurement station is shown in Fig. 4.

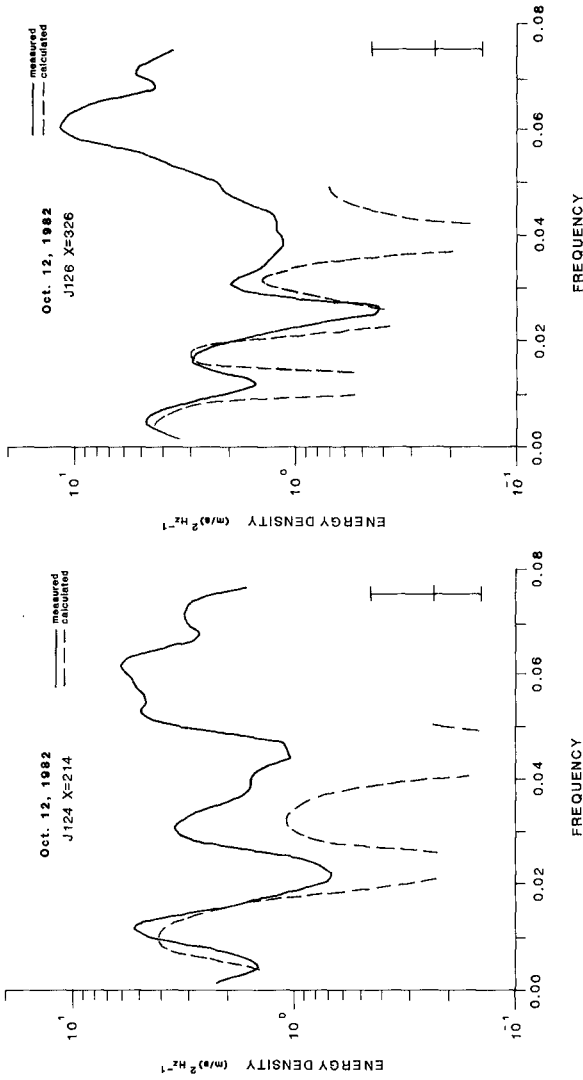


Figure 3. Surf-zone spectra from October 12, 1982. X indicates distance offshore in meters from a baseline; the shoreline relative to this baseline is about 110 m. The number preceded by the J is the run number. 95% confidence limits are shown. The location of each measurement station is shown in Fig. 4.

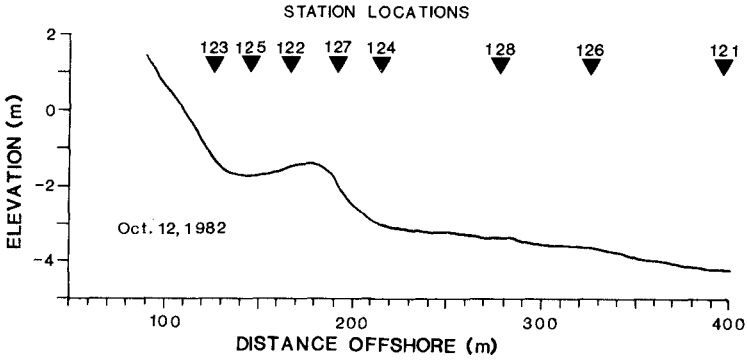


Figure 4. Station locations for October 12. The numbers refer to the J numbers shown on the spectra of Figures 2 and 3.

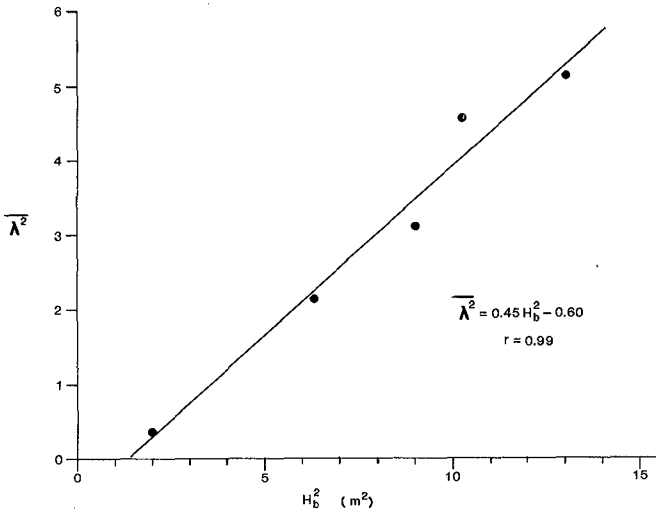


Figure 6. Nondimensional cross-shore flow variances of the infragravity band, λ^2 equation 2, averaged for all offshore positions for a given day are dotted against the square of the breaker height.

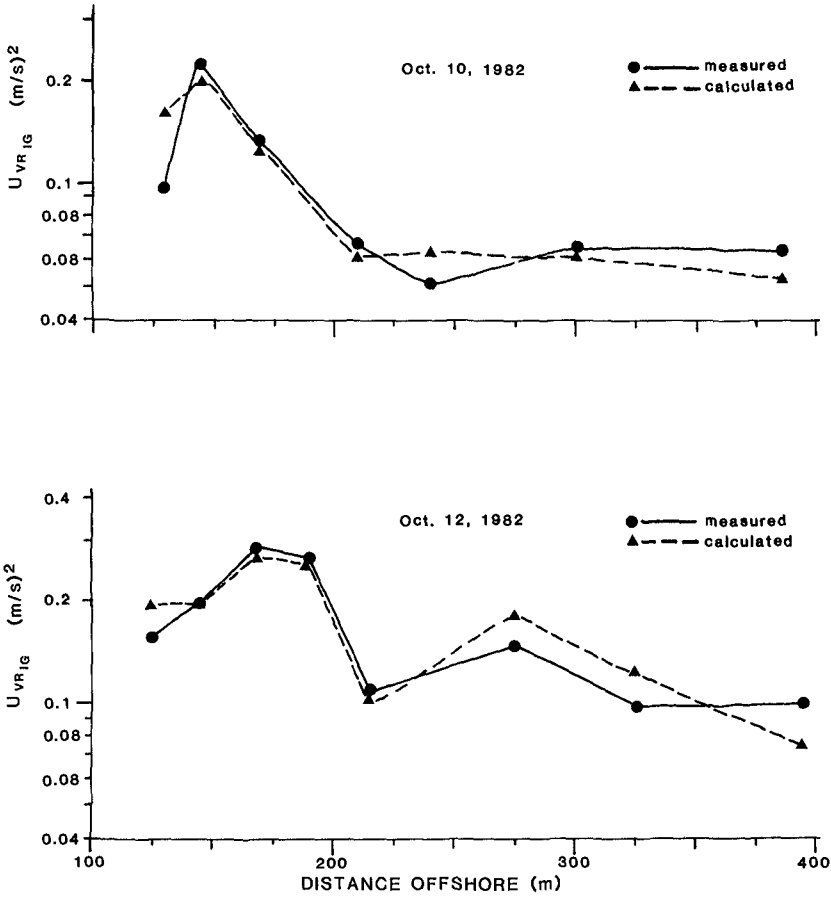


Figure 5. Measured and synthetic variances of the infragravity band. Synthetic variances are defined by equation 4. Measured variances are defined by the numerator of equation 2.

Discussion

Recall that for λ^2 to be applicable, the shoreline spectrum should be white, although we have shown in the discussion of the spectra that the runup spectrum was not white. The implication is that nondimensionalizing cross-shore flow variance, as done in equation 2, is reasonable when the runup spectrum has significant energy across the infragravity band even when that energy is not perfectly white.

It should be interesting to add additional data to Figure 6 to determine whether the relationship is similar for other morphologies and other beaches. However, since we plot against a dimensional quantity in Figure 6 the universal applicability of equation 4 is probably limited. As an alternative, we have plotted the dimensionless Iribarren number, ξ_0 (equation 1) which seems to parameterize many surf zone processes, against λ^2 , but the correspondence is not as good as with H_b^2 (correlation coefficient of 0.56 compared to 0.99).

Knowing the shape of the profile and the breaker height, one can calculate reasonably well the flow due to infragravity waves in the surf zone, at least for the location studied. Since we can also calculate the RMS cross-shore flow in the incident band, incident waves being limited by depth in the surf zone, we can estimate the total oscillatory velocity field. The calculation of total oscillatory flow should be useful for numerical modelers who usually focus on modeling only incident band flows and waves. It should also be useful for sediment transport applications.

Conclusions

1. U_{rms} due to infragravity waves was maximum over the bar crest where it exceeded 0.5 m/s. Cross-shore flow variance due to infragravity waves approached or, in places, exceeded variance in the incident band.

2. As in some earlier studies, calculated spectra, based on a white runup spectrum compared reasonably well with measured spectra.

3. Cross-shore flow variance due to waves in the infragravity band were nondimensionalized by dividing by computed variances based on a white runup spectrum. The nondimensional variances increased with the square of the offshore breaker height.

Acknowledgments

We thank the many persons who contributed to the success of the DUCK82 experiment including Jeff List, Tom Reiss, Peter Howd, Bruce Richmond, Bruce Jaffe, Beth Laband, and the U.S. Army Corps of Engineers crew at the Field Research Facility. We thank David Barnes for doing most of the calculations reported in this paper. Our part of the experiment and the data analysis were funded jointly by the

U.S. Geological Survey and the U.S. Army Corps of Engineers Waterways Experiment Station.

References

- Bowen, A. J., 1980, Simple models of nearshore sedimentation: beach profiles and longshore bars. In: S. B. McCann (Ed.), *Coastline of Canada, Littoral Processes and Shore Morphology*, Geol. Surv. Can., Pap. 80-10, p. 1-11.
- Bowen, A. J., Inman, D. L., 1971, Edge waves and crescentic bars, *J. Geophys. Res.* 76, 8662-8671.
- Guza, R. T. and Thornton, E. B., 1981, Wave setup on a natural beach, *J. Geophys. Res.* 86(c5), 4133-4137.
- Holman, R. A., 1981, Infragravity energy in the surf zone, *J. Geophys. Res.* 86(c7), 6422-6450.
- Holman, R. A., Huntley, D. A., and Bowen, A. J., 1978, Infragravity waves in storm conditions, *Proc. 16th Coastal Eng. Conf.*, p. 268-284.
- Holman, R. A. and Sallenger, A. H., in press, Setup and swash on a natural beach, *J. Geophys. Res.*
- Komar, P. D. and Gaughan, M. K., 1973, Airy wave theory and breaker height prediction, *Proc. 13th Conf. Coastal Eng., Am. Soc. Civ. Eng.*, p. 405-418.
- Mason, C., Sallenger, A. H., Holman, R. A., and Birkemeier, W. A., in press, DUCK82 - A coastal storm processes experiment, *Proc. 19th Coastal Engineering Conference, Am. Soc. Civ. Eng.*
- Sallenger, A. H., Holman, R. A., and Birkemeier, W. A., in press, Storm response of a nearshore bar system, *Marine Geology*.
- Sallenger, A. H., Howard, P. C., Fletcher, C. H., and Howd, P. A., 1983, A system for measuring bottom profile, waves and currents in the high-energy nearshore environment, *Marine Geology*, 51, p. 63-76.
- Suhayda, J. N., 1974, Standing waves on beaches, *J. Geophys. Res.* 72, 3065-3071.
- Wright, L. D., Chappell, J., Thom, B. G., Bradshaw, M. P., and Cowell, P., 1979, Morphodynamics of reflective and dissipative beach and nearshore systems: southeastern Australia, *Marine Geology*, 32, 105-140.
- Wright, L. D., Guza, R. T., Short, A. D., 1982, Dynamics of a high energy dissipative surf zone, *Marine Geology*, v. 45, p. 41-62.